

Received: 2019.11.20

Accepted: 2020.02.12

Available online: 2020.02.24

Published: 2020.03.03

# Establishment and Simulation of 3D Geometric Models of Mini-Pig and Sheep Knee Joints Using Finite Element Analysis

Authors' Contribution:  
Study Design A  
Data Collection B  
Statistical Analysis C  
Data Interpretation D  
Manuscript Preparation E  
Literature Search F  
Funds Collection G

BC 1 **Peng-fei Han\***  
BC 2 **Rong Zhang\***  
D 3 **Yang-yang Gao**  
EG 3 **Peng-cui Li**  
FG 3 **Xiao-chun Wei**  
A 3 **Zhi Lv**

1 Department of Orthopaedics, Heping Hospital Affiliated to Changzhi Medical College, Changzhi, Shanxi, P.R. China  
2 Department of Oncology, Heping Hospital Affiliated to Changzhi Medical College, Changzhi, Shanxi, P.R. China  
3 Department of Orthopaedics, The Second Hospital of Shanxi Medical University, Shanxi Key Laboratory of Bone and Soft Tissue Injury Repair, Taiyuan, Shanxi, P.R. China

\* Peng-fei Han and Rong Zhang were considered as co-first authors

**Corresponding Author:** Zhi Lv, e-mail: 18035526520@163.com

**Source of support:** This study was supported by the National Project of International Science and Technology Cooperation Program of China (2015DFA33050) and the National Natural Science Foundation of China (81601949)

**Background:** Our objective was to establish and compare three-dimensional models of knee joints of mini-pigs and sheep, the 2 most commonly used animal models of osteoarthritis.


**Material/Methods:** Three-dimensional geometric models of knee joints were used to assess their biomechanical properties by analysis of the three-dimensional finite element stress load for flexion at 30° and 60°.

**Results:** Analysis of multiple tissues indicated that the sheep knee had greater stress peaks than the mini-pig knee at 30° flexion (range: 12.5 to 30.4 Mpa for sheep vs. 11.1 to 20.2 Mpa for mini-pig) and at 60° flexion (range: 17.9 to 43.5 Mpa for sheep vs. 15.9 to 28.9 Mpa for mini-pig). In addition, there was uneven distribution of stress loads in the surrounding ligaments during flexion.

**Conclusions:** Our three-dimensional finite element analysis indicated that the mini-pig knee joint had stress values and changes of cartilage, meniscus, and peripheral ligaments that were similar to those of the human knee.

**MeSH Keywords:** **Anterior Cruciate Ligament • Finite Element Analysis • Imaging, Three-Dimensional • Sheep • Swine, Miniature**

**Full-text PDF:** <https://www.medscimonit.com/abstract/index/idArt/921540>

 2357

 3

 14

 32



## Background

Researchers commonly use sheep and mini-pigs as animal models of human diseases because of their similarities to humans [1]. In particular, mini-pigs have physiological and serum biochemical parameters that are similar to those of humans, and their peripheral bone deposition rate and trabecular density are also similar to those of humans [2]. Moreover, the arrangement of the collagen fibers of cartilage tissue is similar in mini-pigs and humans, in contrast to the columnar arrangement pattern present in other common experimental animals, such as rats, rabbits, and dogs [3]. Therefore, researchers have increasingly used mini-pigs for experimental animal research since the 1970s [4].

Researchers presently use mini-pigs as models for research on many topics, such as the cardiovascular system, the digestive system, the urinary system, skin burns, stomatology, pharmacology, and toxicology [5]. In the past decade, numerous pre-clinical studies in orthopedics have used mini-pigs as animal models for bone research. The orthopedic properties of mini-pigs are similar to those of humans in terms of gross morphology [6], composition [7], microstructure [8], and remodeling characteristics [9].

However, it is unknown whether the knee of the mini-pig is biomechanically similar to the human knee. Our literature search indicated that no previous studies have established a digital geometric model for analysis of the biomechanical properties of the intact mini-pig knee joint, including the meniscus, articular cartilage, and peripheral ligaments, such as the anterior and posterior cruciate ligaments, medial and lateral collateral ligaments, and other tissues.

Finite element analysis is a mathematical technique that can be used to simulate biomechanical properties, such as different loads and stresses experienced by the body, by use of a digital geometric model. In particular, three-dimensional finite element analysis [10–12] can accurately control for variations of experimental conditions, in contrast to traditional experimental methods with living animals, and thereby provide more accurate characterizations of body mechanics. Researchers first applied this method in 1972 to perform a stress analysis of bones, and this initial research pioneered its application to the field of medical research [13,14]. In recent years, with improvements of computer technologies, three-dimensional finite element analysis has rapidly developed due to its unparalleled advantages in the examination of three-dimensional structural mechanics, and has received increasing attention from researchers. Researchers are currently using this technology for analysis of the biomechanical properties of bone, cartilage, and ligaments [15–17].

In this study, we first obtained image data by scanning the knee joints of mini-pigs using micro-computed tomography (micro-CT), and then used finite element analysis software, including Mimics and Nastran, to establish a high-quality three-dimensional digital geometric model of the knee. We then applied this model to assess the biomechanical load distribution under conditions of 30° flexion and 60° flexion, angles at which the anterior cruciate ligament is in a relaxed state and more vulnerable to external forces. We used sheep, another commonly used animal model, as a control species.

## Material and Methods

All procedures used for animal surgery and pre- and post-operative care were approved by the Ethics Committee of the Second Hospital of Shanxi Medical University (no. 2017046). All relevant animal protection agreements and regulations were followed. The adult mini-pigs (18 months old, female) and sheep (8 months old, female) were purchased from Beijing Shichuang Century Breeding Base. High-resolution micro-CT (Viva CT 80, Scanco Medical AG, Switzerland) was used for imaging.

### Establishment of geometric models of the mini-pig and sheep knee joints

#### 3D reconstruction

The specific procedure used for three-dimensional reconstruction of the knee joints of the mini-pig and sheep had 4 general steps. First, a tomographic image (DICOM format) was obtained by micro-CT of the posterior right knee joints of a mini-pig and a sheep. Neither animal had knee joint disease, trauma, or a history of surgery.

Second, Mimics software (version 16.0) was used to transform and process the data of the two-dimensional tomographic images to reconstruct geometric models of the knee joints and to export these 3D files in STL format. In this process, DICOM data were imported into Mimics software, and the view direction was set. The coronal, sagittal, and cross-sections were defined, and the DICOM image data were arrayed in order. Grayscale images of the knee joints and background were obtained from the interface.

Gray values were derived from tissues with different densities. According to the different gray values (tissue density), the “threshold” command was used to set the corresponding gray threshold interval, and the structural tissues of each knee joint were extracted. The rough geometric model of the knees was saved as STL files.

Third, the STL files were processed using Geomagic Studio 2014 software by use of subdivided noise reduction and smoothing. Then, a series of processes was used to fit the surface. Finally, three-dimensional solid models of the intact knee joints were obtained and saved as STP files.

Fourth, the knee joint models were supplemented in structure and reconstructed using Pro/Engineer 5.0 software. These models included the femur, tibia, fibula, patella, articular cartilage, meniscus, and other key tissues. The surrounding ligaments (anterior and posterior cruciate ligaments, the medial lateral collateral ligaments, and the patellar tendons) were one-dimensional models and considered as nonlinear spring elements. Finally, the intact knee joint models were exported as IGES files (Figures 1–4).

#### Finite element meshing

The IGES files for the knee joints were then analyzed using Hypermesh 13.0 software. This software provided 29 393 nodes with 136 143 tetrahedral units for the mini-pig knee, and 42 702 nodes with 199 909 tetrahedral units for the sheep knee. The solid skeleton mesh was used for the knee joint structure, articular cartilage, and meniscus, and a one-dimensional

nonlinear spring element mesh was used for the surrounding ligament. The resulting BDF files were ultimately exported (Figures 5–8). Eventually, finite element analysis was performed using MSC Nastran 2012 software.

#### Material parameter settings

Results from previous studies [18,19] were used to establish the material properties of each structure or tissue of the mini-pig and sheep knee joints. The load frequency of articular cartilage, meniscus, and other tissues is generally greater than 0.1 Hz during daily activities (e.g., walking and going up and down stairs), and their structure remains in the elastic phase, so they were all considered to be elastic materials [20] (Table 1). Compared with the three-dimensional solid element, the one-dimensional spring unit better characterizes the biomechanical properties of each ligament. Hence, the surrounding ligaments in this study model were simplified as a one-dimensional nonlinear spring element (Table 2). In addition, the frictional contact mode was used between the meniscus and the articular cartilage, and the friction coefficient was set to 0.2 [21]. The counterparts of the other structures were common node contacts.



**Figure 1.** Geometric model of the mini-pig knee in posterior (**top**) and lateral (**bottom**) views, showing the bone (**left**), articular cartilage (**middle**), and peripheral ligament and meniscus (**right**).

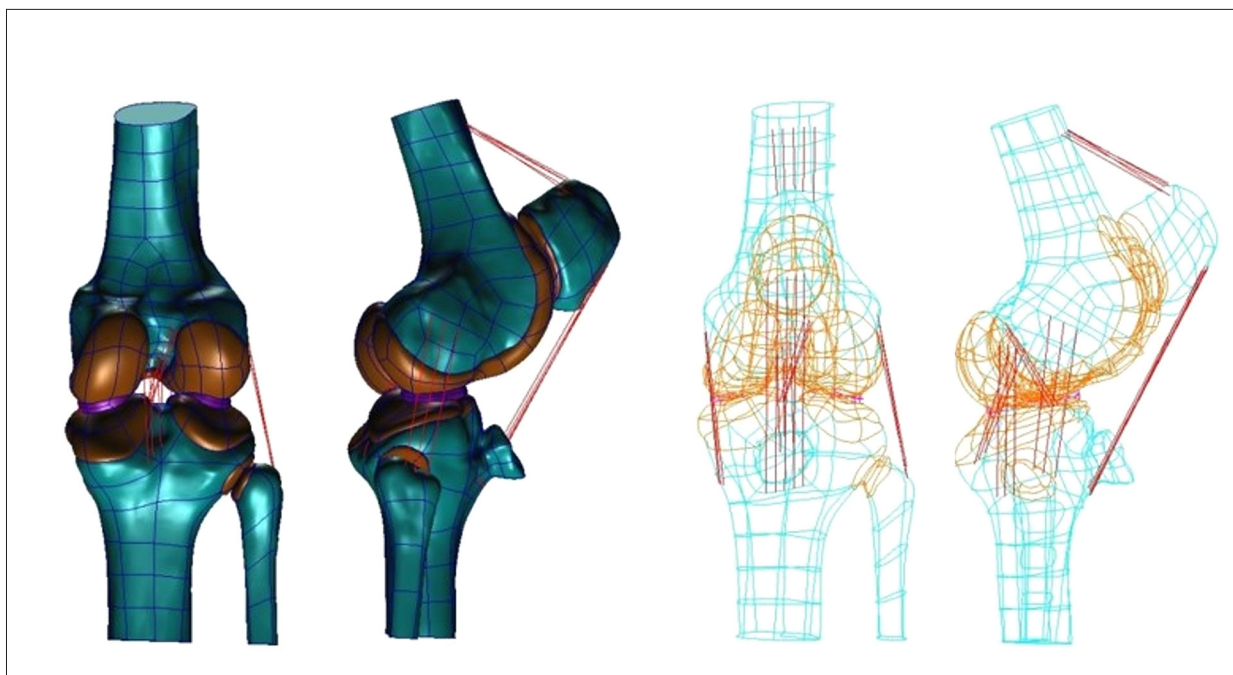


**Figure 2.** Overall geometric model (**left**) and shadow map (**right**) of the mini-pig knee in posterior and lateral views.

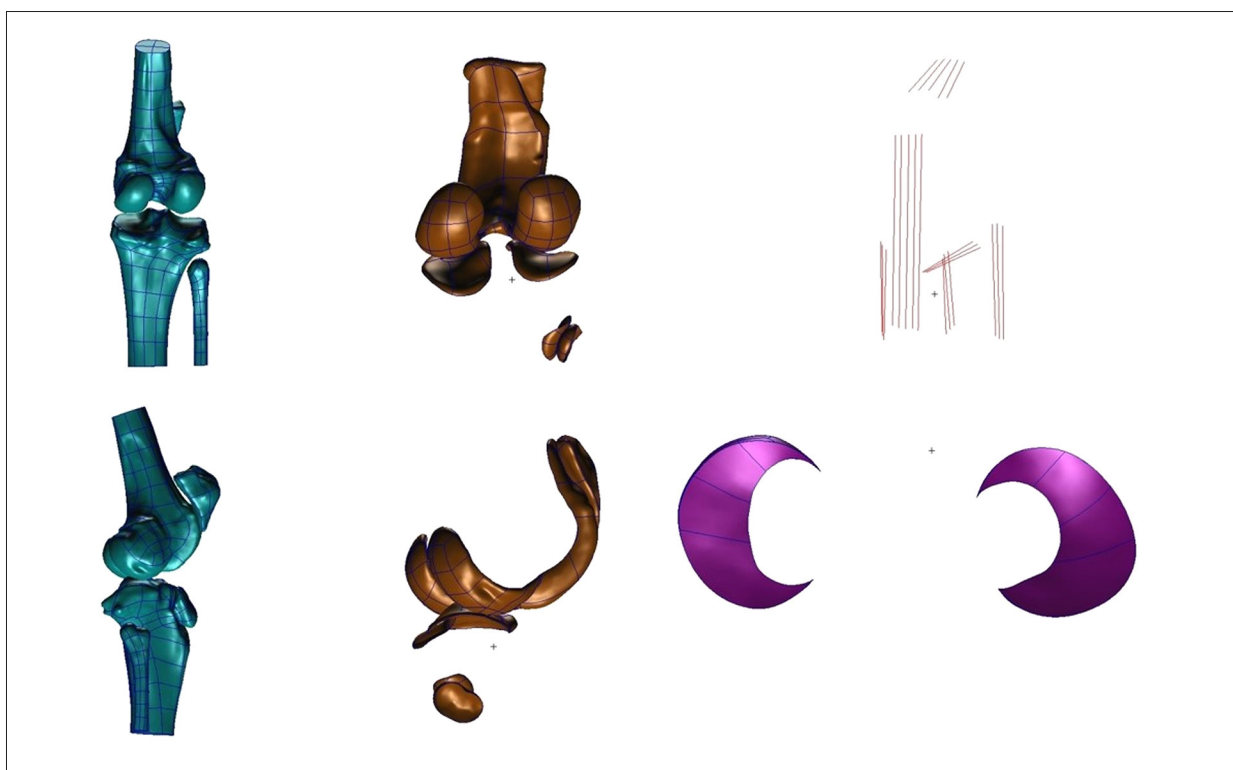


**Figure 3.** Geometric model of the sheep knee in posterior and lateral views, showing the bone (**left**), articular cartilage (**middle**), and peripheral ligament and meniscus (**right**).



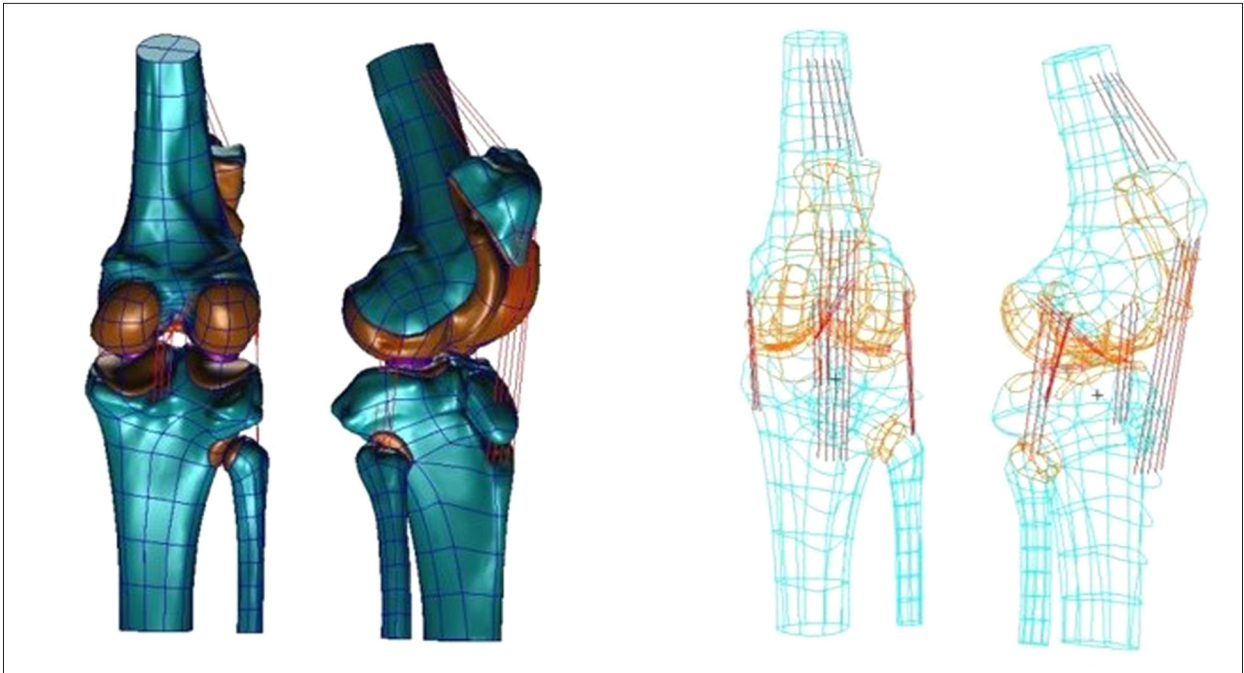


**Figure 4.** Overall geometric model (**left**) and shadow map (**right**) of the sheep knee in posterior and lateral views.

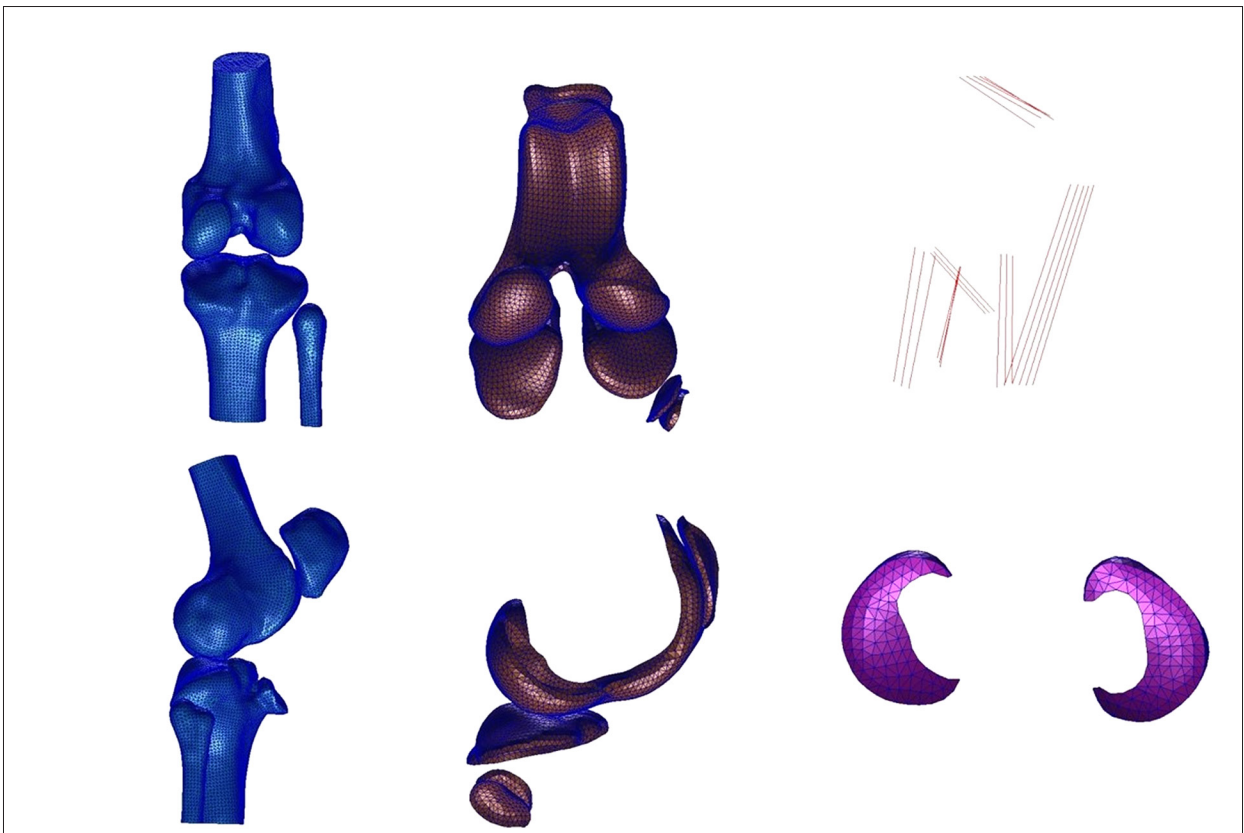


**Figure 5.** Finite element mesh model of the mini-pig knee joints in posterior and lateral views, showing the bone (**left**), articular cartilage (**middle**), and peripheral ligament and meniscus (**right**).

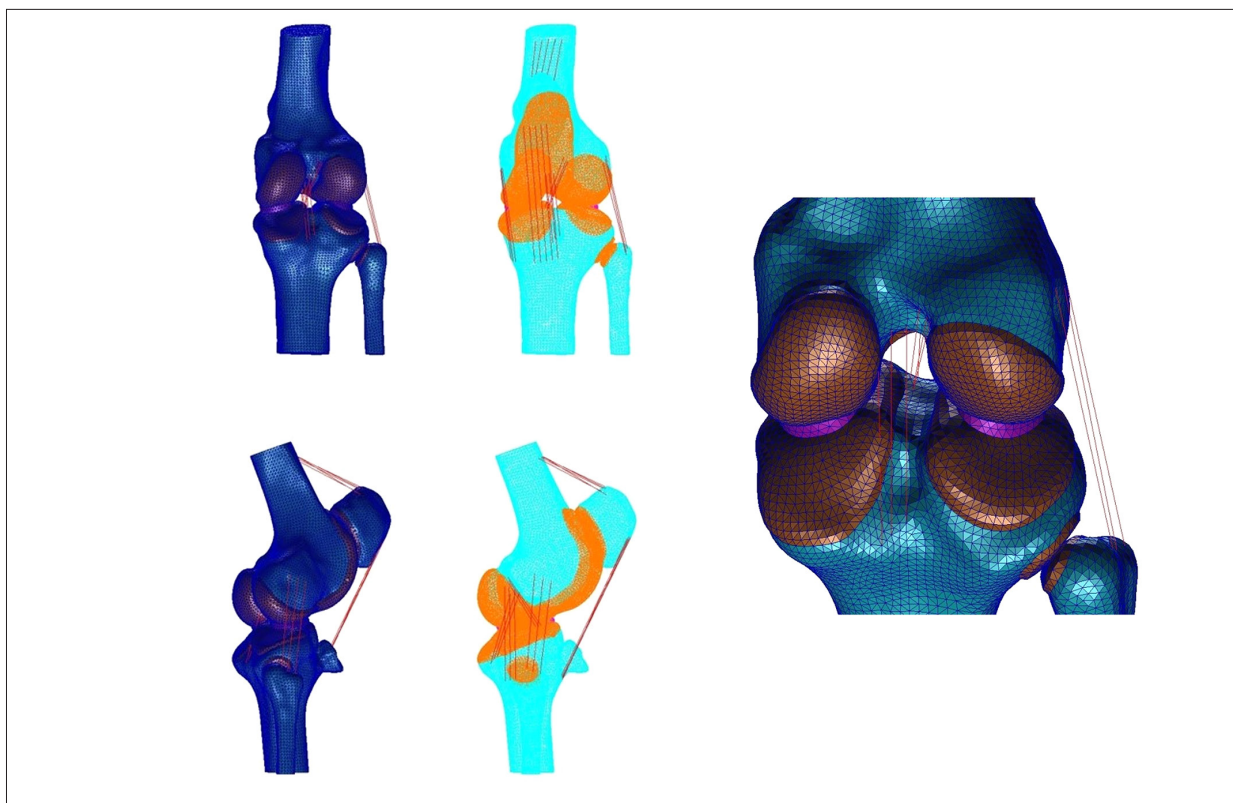


**Figure 6.** Overall mesh model of the mini-pig knee joints (**left**) and shadow map (**middle**) in posterior and lateral views, and local grid details (**right**).



**Figure 7.** Finite element mesh model of the sheep knee joints in posterior and lateral views, showing the bone (**left**), articular cartilage (**middle**), and peripheral ligament and meniscus (**right**).

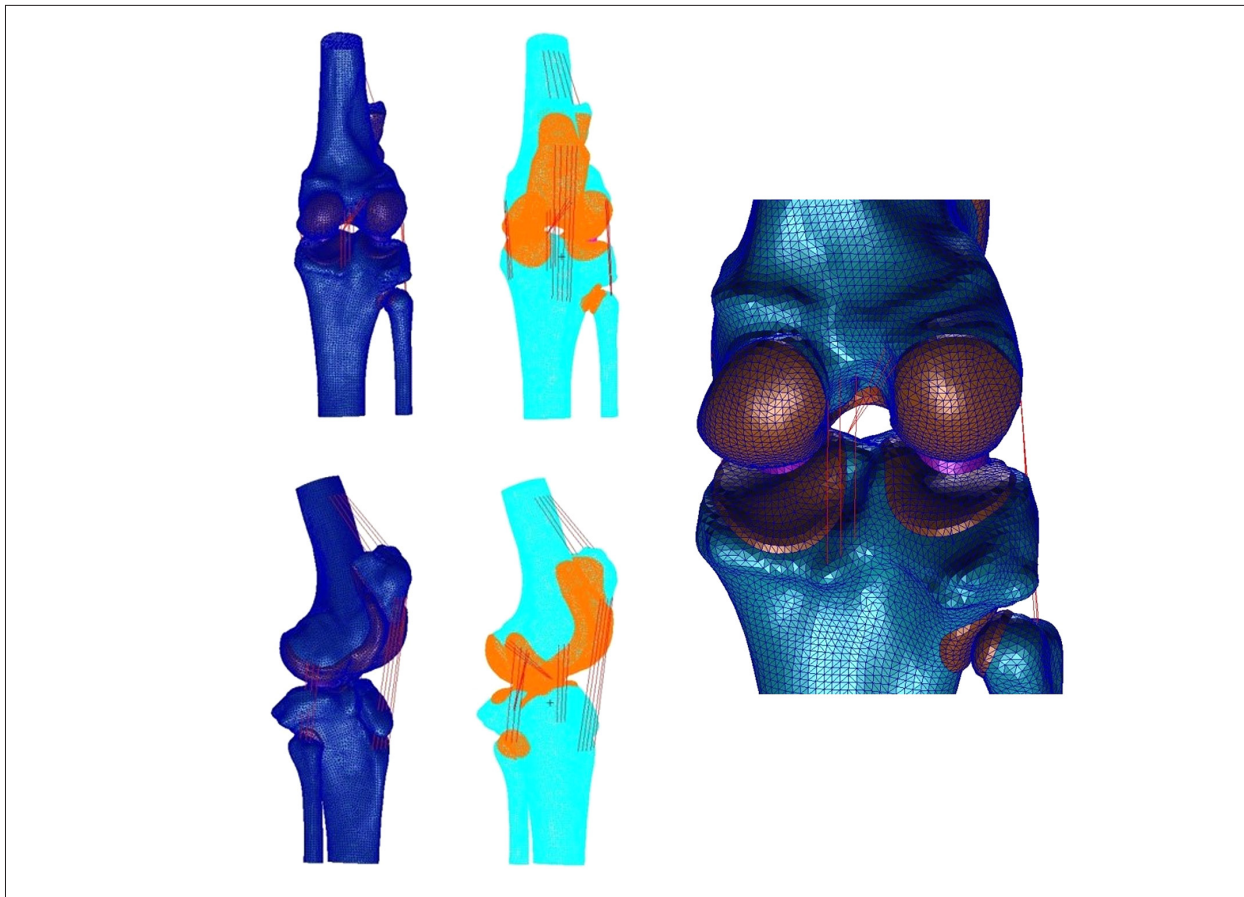


**Figure 8.** Overall mesh model of the sheep knee joints (**left**) and shadow map (**middle**) in posterior and lateral views, and local grid details (**right**).

**Table 1.** Material parameters of the mini-pig knee joint structures, articular cartilage, and meniscus.

Structure	Modulus of elasticity (MPa)	Poisson's ratio
Femur	3883.4	0.30
Patella	3883.4	0.30
Humerus	4184.6	0.30
Fibula	4184.6	0.30
Articular cartilage	5	0.46
Meniscus	59	0.49

### Boundary conditions

There were several boundary conditions used for modeling the mini-pig and sheep knee joints (Figure 9). First, the cross-sections of the tibia and fibula were fixed, then all nodes on the lower surface of the tibia and fibula were constrained, thus limiting the degrees of freedom (DOF) to 6 directions. However,

**Table 2.** Material parameters of the mini-pig knee joint ligaments as a nonlinear spring unit.

Structure	Bulk modulus, K (N/mm)
Anterior cruciate ligament	125
Posterior cruciate ligament	125
Medial collateral ligament	27.9
Lateral collateral ligament	91.3
Patellar ligament	300

the upper end of the femur was unconstrained. Second, the skeletal structure, articular cartilage, and meniscus were assumed to be isotropic, homogeneous, and continuous elastic materials because of the complex nature of the skeletal tissue and the limitations of the experimental conditions. Third, all ligaments were assumed to be one-dimensional nonlinear spring units and were defined as elastoplastic materials. Fourth, because the upper end of the femur is cut off, all nodes of the femoral section were coupled to a reference point when the load was applied. The moment load was directly applied to

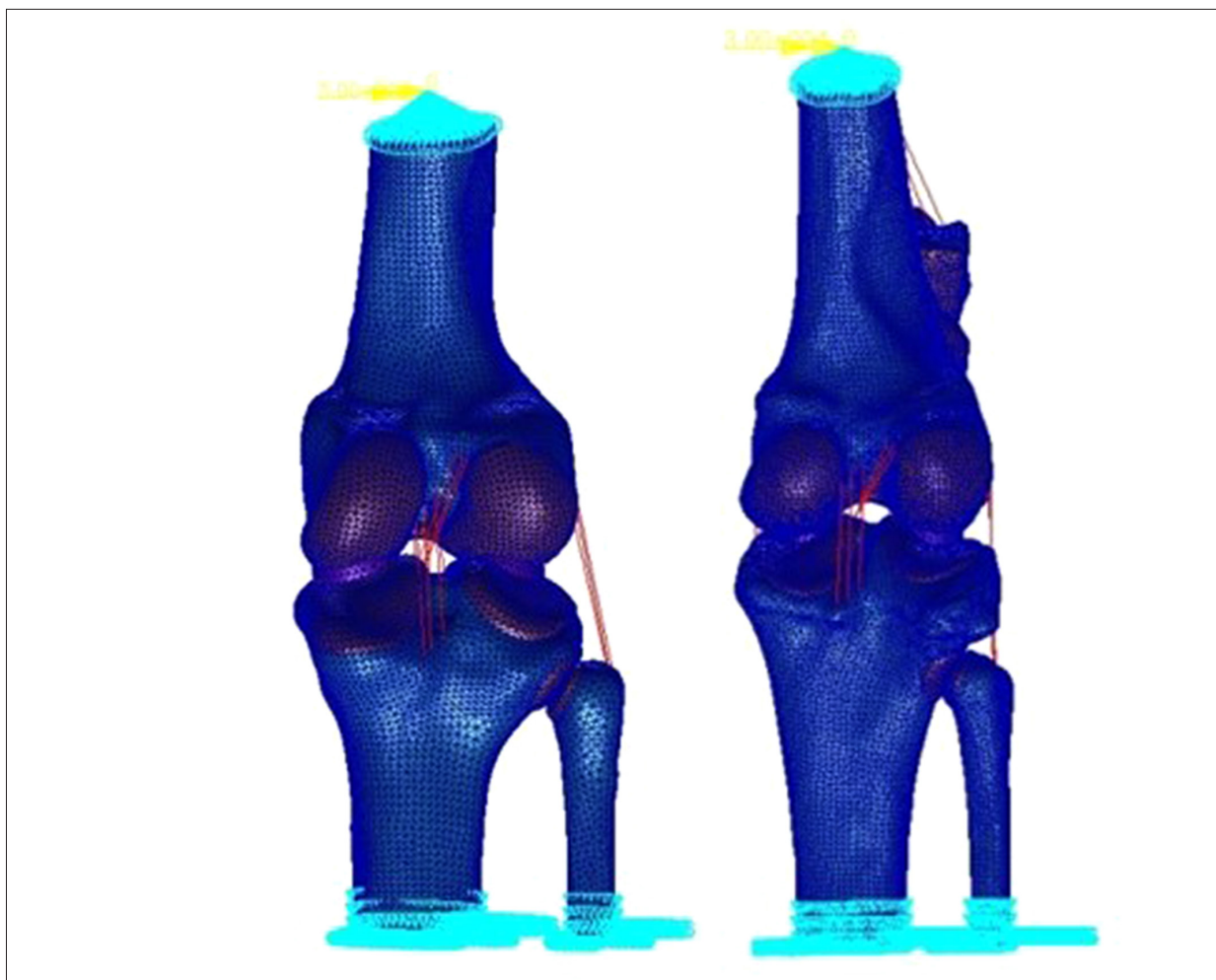


**Figure 9.** Posterior views of the knee of the mini-pig (left) and sheep (right), showing boundary conditions and load application.

the reference point (torque=30 N·m for 30° flexion; torque=43 N·m for 60° flexion [22]), which made the load transfer more uniform and reliable, and also simulated changes in the biomechanical properties of the knee joint tissues under different flexion angles.

#### **Biomechanical study and finite element analysis of mini-pig and sheep knees**

Finite element analysis provided a von Mises stress map for the different tissues of the knee joints of the mini-pigs (Figures 10, 11) and the sheep (Figures 12, 13) at flexion angles of 30° and 60°.

## **Results**

We used finite element analysis to determine the von Mises stress peaks for the different parts of the knee joints of the mini-pig and sheep under conditions of flexion of 30° and

60° (Table 3, Figure 14). Used finite element analysis to determine the von Mises stress peaks for the medial and lateral meniscus, internal and external femoral cartilage, medial and lateral cartilage of the tibial plateau, anterior and posterior cruciate ligament, and medial lateral collateral ligament and iliac crest ligament in sheep knee joints with knee flexion 30° and knee flexion 60° moment load, (Table 3). In particular, the stress peaks of the meniscus and the femoral and tibial articular cartilage of the mini-pig knee joints were between 11.1 and 20.2 MPa at 30° flexion and between 15.9 and 28.9 MPa at 60° flexion, respectively. The stress on each tissue structure increased as flexion increased. Thus, compared with flexion of 30°, the structural stress of the meniscus and cartilage was approximately 43% greater at a flexion of 60°. A histogram is drawn based on the data in the table to compare the stress in knee joints of mini-pigs and sheep in every structure, as shown in Figure 14.



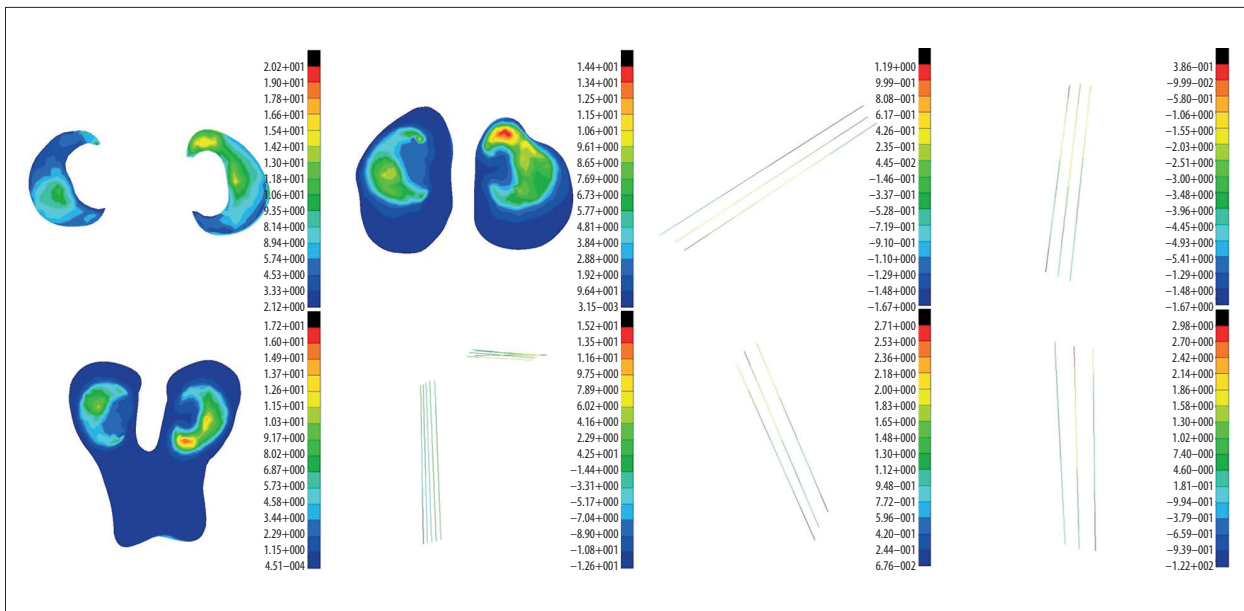


**Figure 10.** Stress diagrams of each structure of the mini-pig knee joints at 30° flexion. From left to right: small (**top**) and medium (**bottom**) internal meniscus; internal (**top**) and external (**bottom**) femoral cartilage; medial and lateral cartilage of the tibial plateau, patellar tendon, anterior cruciate ligament, posterior cruciate ligament, the medial collateral ligament and the lateral side.

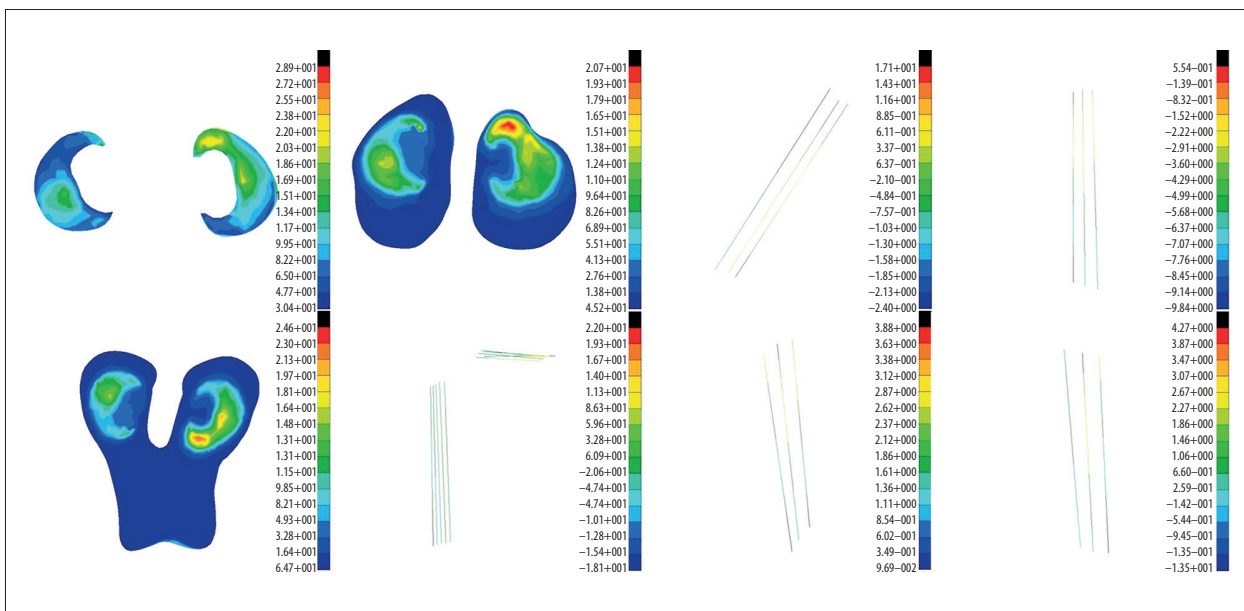


**Figure 11.** Stress diagrams of each structure of the mini-pig knee joints at a 60° flexion. See Figure 10 for further details.

## Discussion

It is well known that the ligaments of the knee joint play a more critical role in maintaining joint stability than does the skeletal structure. The knee is the joint that has the largest volume and bears the most weight in the human body. However, due to its morphological and structural characteristics, knee joints are unstable, and knee joint damage, especially ligament injury,

is a very common clinical condition [23,24]. Therefore, many researchers of knee biomechanics have focused their studies on the surrounding ligaments of the knee.

Three-dimensional finite element analysis has developed rapidly due to its unparalleled advantages in characterizing structural mechanics in 3 dimensions. The use of finite element analysis for biomechanical simulation can characterize load

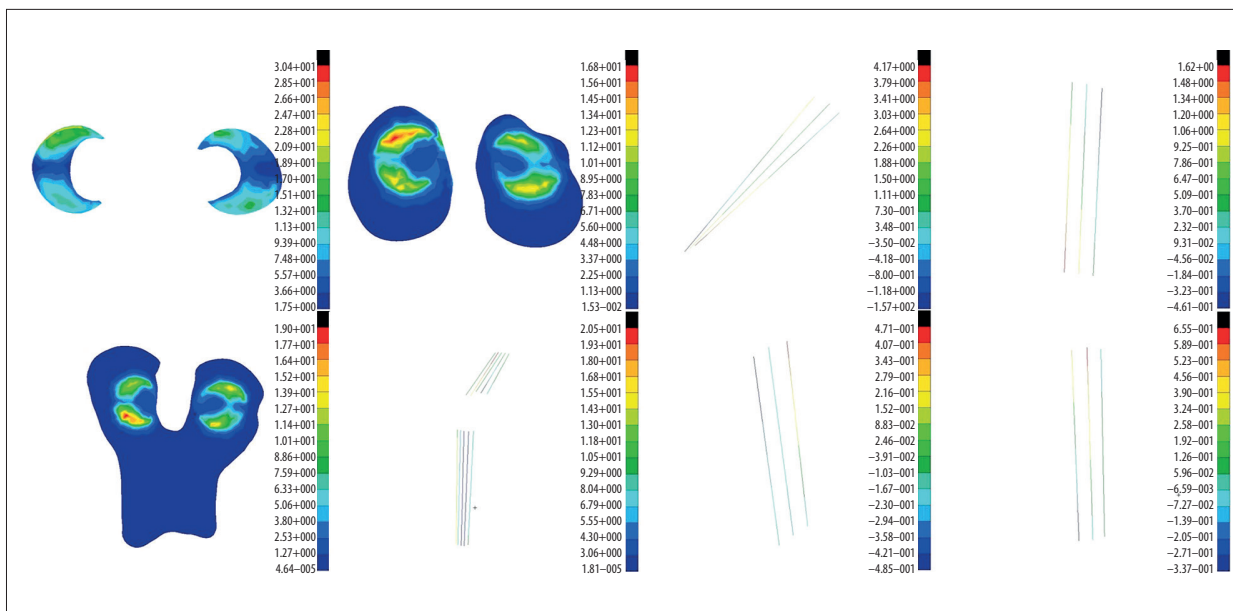


Figure 12. Stress diagrams of each structure of the sheep knee joints at 30° flexion. See Figure 10 for further details.

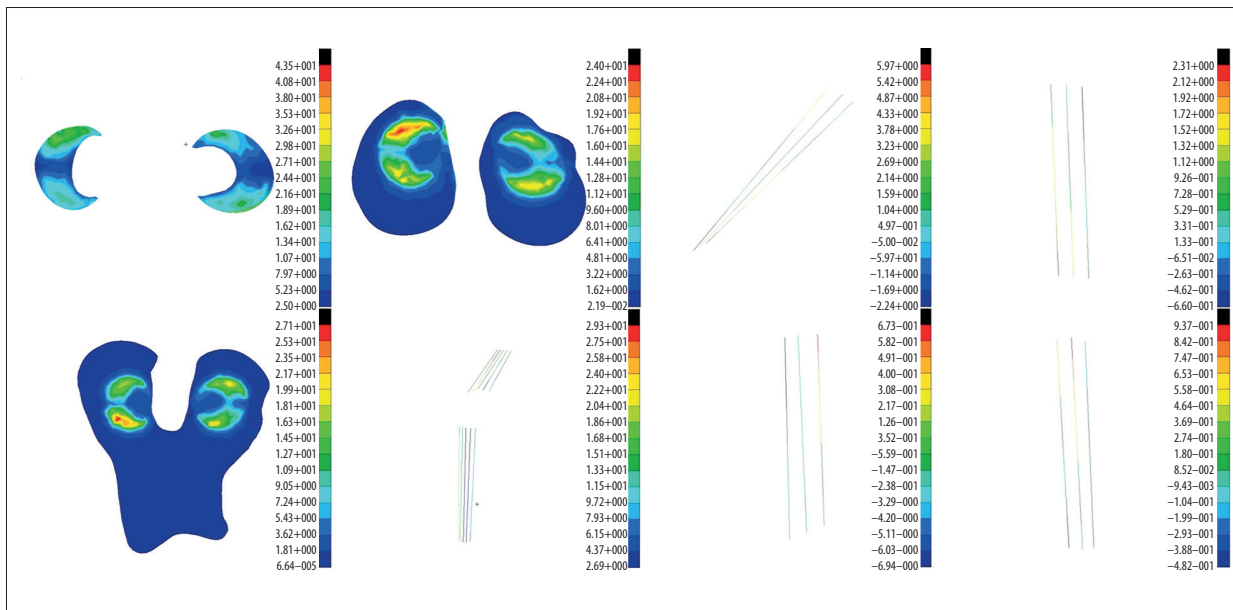


Figure 13. Stress diagrams of each structure of the sheep knee joints at 60° flexion. See Figure 10 for further details.

and stress by establishing a digital geometric model. Finite element analysis, especially three-dimensional finite element analysis [25,26], can also more accurately control for variations that normally occur during traditional experimental conditions, and therefore provides a more accurate characterization of the mechanics of the body. This method was first applied to the stress analysis of bones in 1972, and it has subsequently transformed the field of biomechanics [27]. Improvements in computing hardware and software have enabled the rapid development of three-dimensional finite element analysis, and this method now has unparalleled advantages in examining

three-dimensional structural biomechanics. Thus, this technology is now widely used for the analysis of the biomechanical properties of bone, cartilage, and ligaments [28–30].

It is important to have an animal model for studies of ACL injury and reconstruction that is similar to humans. Thus, previous studies have examined mini-pigs and sheep. We performed a qualitative and quantitative biomechanical study of the knees of the mini-pig and sheep using three-dimensional finite element analysis, and then applied mechanical principles and structural engineering theory to conduct three-dimensional

**Table 3.** Structural stress peaks of the knee joints of the mini-pig and sheep at flexions of 30° and 60°.

Structure	Mini-pig knee stress (MPa)		Sheep knee stress (MPa)	
	Flexion 30°	Flexion 60°	Flexion 30°	Flexion 60°
Medial meniscus	13.2	19.0	30.4	43.5
Lateral meniscus	20.2	28.9	26.6	38.1
Cartilage of medial femoral condyle	11.5	16.4	19.0	27.1
Cartilage of lateral femoral condyle	17.2	24.6	15.2	21.7
Cartilage of medial tibial plateau	11.1	15.9	16.8	24.0
Cartilage of lateral tibial plateau	14.4	20.7	12.5	17.9
Anterior cruciate ligament	1.19	1.71	4.17	5.97
Posterior cruciate ligament	2.71	3.88	0.47	0.67
Medial collateral ligament	0.39	0.55	1.62	2.31
Lateral collateral ligament	2.98	4.27	0.66	0.94
Patellar ligament	15.3	22.0	20.5	29.3

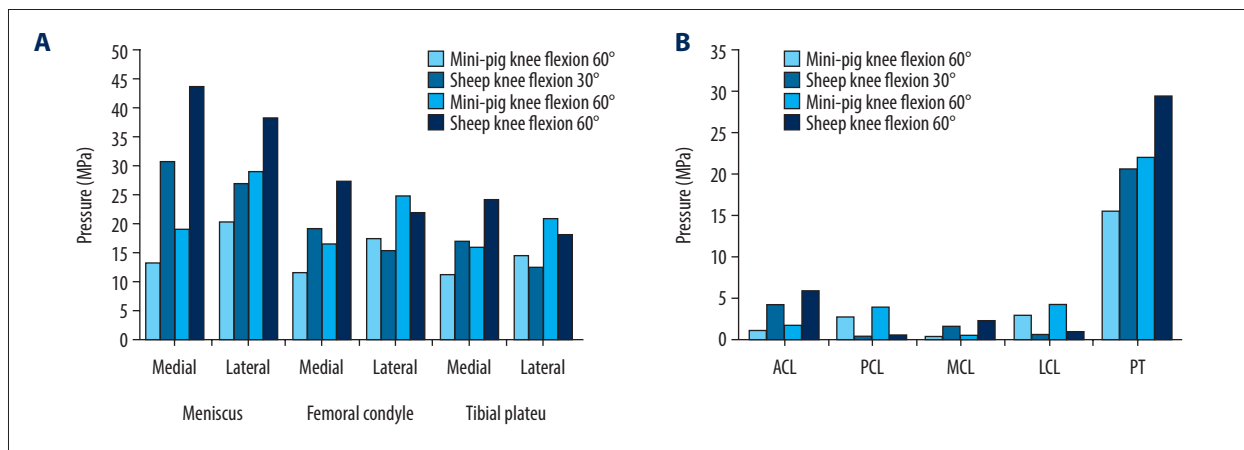


**Figure 14.** Structural stress peaks of the knee joints of the mini-pig and sheep at flexions of 30° and 60°. (A) Meniscus/cartilage stress, (B) ligament stress.

simulations of these 2 animal knee joints. Finally, we compared our animal results with the results of previous studies of human knee joints to identify the animal model that is most similar to humans.

We first used micro-CT image reconstruction technology to develop models of the skeletal structure of the knees of the mini-pig and sheep in 3 dimensions. We then added soft tissue structures (articular cartilage, meniscus, anterior and posterior cruciate ligament, medial lateral collateral ligament, and patella ligament) using a reverse processing technique, and finite element analysis for analysis at 30° and 60° flexion. Finally, our data indicated that the outer structure of the knee joint of the mini-pig was generally more stressed than the inner structure under conditions of different flexion.

We also determined the peak stress of the surrounding ligaments of the mini-pig knee joints. The results indicated that the stress of the patella ligament was much greater than that of other ligaments, thus reflecting the stiffness of the patella ligament itself and the large stretch of this ligament during flexion. In particular, the stress peak of the patella ligament was 15.3 MPa at 30° flexion and 22 MPa at 60° flexion, similar to the values reported for human knees; the stress peaks of the remaining ligaments were between 0.39 and 2.98 MPa at 30° flexion and between 0.55 and 4.27 MPa at 60° flexion. The posterior cruciate ligament had greater stress than the anterior cruciate ligament, and the lateral collateral ligament had greater stress than the medial collateral ligament.

In contrast, our data for sheep knee joints indicated that the medial structure was more stressed than the lateral structure at different flexion angles. The stress peaks of the meniscus

and the femoral and the tibial articular cartilage of the sheep knee joints were between 12.5 and 30.4 MPa at 30° flexion and between 17.9 and 43.5 MPa at 60° flexion. Thus, for the same flexion angle, the stress peaks were greater for the various structures of the knee joints of sheep than the mini-pig. Although the stress on the lateral cartilage of the femoral condyle and the lateral cartilage of the tibial plateau were less than in the mini-pig, this difference was below 13%. For different flexion angles, except for the patella ligament, the stress peaks of the peripheral ligaments of the sheep knee joints were between 0.47 and 4.17 MPa at 30° flexion and between 0.67 and 5.97 MPa at 60° flexion. In addition, the sheep knee had much greater stress on the anterior cruciate and medial collateral ligaments than on the posterior cruciate and lateral collateral ligaments.

## References:

- Bassols A, Costa C, Eckersall PD et al: The pig as an animal model for human pathologies: A proteomics perspective. *Proteomics Clin Appl*, 2014; 8(9–10): 715–31
- Ramos L, Obregon-Henao A, Henao-Tamayo M et al: The minipig as an animal model to study *Mycobacterium tuberculosis* infection and natural transmission. *Tuberculosis (Edinb)*, 2017; 106: 91–98
- Otto S, Pautke C, Martin Jurado O et al: Further development of the MRONJ minipig large animal model. *J Craniomaxillofac Surg*, 2017; 45(9): 1503–14
- Iwatsuki-Horimoto K, Nakajima N, Shibata M et al: The microminipig as an animal model for influenza A virus infection. *J Virol*, 2017; 91(2): pii: e1716-16
- Schulze-Tanzil G, Silawal S, Hoyer M: Anatomical feature of knee joint in Aachen minipig as a novel miniature pig line for experimental research in orthopaedics. *Ann Anat*, 2020; 227: 151411
- Jang Y, Cho I, Hartaigh BWO et al: Viability assessment after conventional coronary angiography using a novel cardiovascular interventional therapeutic CT system: Comparison with gross morphology in a subacute infarct swine model. *J Cardiovasc Comput Tomogr*, 2015; 9(4): 321–28
- Park S, Lee P, Ha W-H et al: Development of a minipig physical phantom from CT data. *J Radiat Res*, 2017; 58(5): 755–60
- Mueller CK, Solcher P, Peisker A et al: Analysis of the influence of the macro- and microstructure of dental zirconium implants on osseointegration: A minipig study. *Oral Surg Oral Med Oral Pathol Oral Radiol*, 2013; 116(1): e1–8
- Zhou W, Kuderer S, Liu Z et al: Peri-implant bone remodeling at the interface of three different implant types: A histomorphometric study in minipigs. *Clin Oral Implants Res*, 2017; 28(11): 1443–49
- Wang J, Qian Z, Ren L: Biomechanical comparison of optimal shapes for the cervical intervertebral fusion cage for C5–C6 cervical fusion using the anterior cervical plate and cage (ACPC) fixation system: A finite element analysis. *Med Sci Monit*, 2019; 25: 8379–88
- Zhang Y, Zhou J, Guo X et al: Biomechanical effect of different graft heights on adjacent segment and graft segment following C4/C5 anterior cruciate discotomy and fusion: a finite element analysis. *Med Sci Monit*, 2019; 25: 4169–75
- Pfeiffer FM: The use of finite element analysis to enhance research and clinical practice in orthopedics. *J Knee Surg*, 2016; 29(2): 149–58
- Hudieb MI, Wakabayashi N, Abu-Hammad OA, Kasugai S: Biomechanical effect of an exposed dental implant's first thread: A three-dimensional finite element analysis study. *Med Sci Monit*, 2019; 25: 3933–40
- Li J, Zhao X, Hu X et al: A theoretical analysis and finite element simulation of fixator-bone system stiffness on healing progression. *J Appl Biomater Funct Mater*, 2018; 16(3): 115–25
- Coombs DJ, Rullkoetter PJ, Laz PJ: Efficient probabilistic finite element analysis of a lumbar motion segment. *J Biomech*, 2017; 61: 65–74
- Cui Y, Hu P, Wei N et al: Finite element study of implant subsidence and medial tilt in agility ankle replacement. *Med Sci Monit*, 2018; 24: 1124–31
- Buhara O, Erkmen E, Orhan K: Displacement patterns of the maxilla during parallel and rotational setback movements: A finite element analysis. *Med Sci Monit*, 2017; 23: 1607–12
- Koh Y-G, Lee J-A, Lee H-Y et al: Design optimization of high tibial osteotomy plates using finite element analysis for improved biomechanical effect. *J Orthop Surg Res*, 2019; 14(1): 219
- Mo F, Zhang H, Zhao S et al: Coupling musculoskeletal dynamics and subject-specific finite element analysis of femoral cortical bone failure after endoprosthetic knee replacement. *Appl Bionics Biomech*, 2019; 2019: 4650405
- Zach L, Kuncicka L, Ruzicka P, Kocich R: Design, analysis and verification of a knee joint oncological prosthesis finite element model. *Comput Biol Med*, 2014; 54: 53–60
- Wu JZ, Herzog W, Hasler EM: Inadequate placement of osteochondral plugs may induce abnormal stress-strain distributions in articular cartilage – finite element simulations. *Med Eng Phys*, 2002; 24(2): 85–97
- Paul JP: Simulation of a knee joint replacement during a gait cycle using explicit finite element analysis. *J Biomech*, 2005; 38(3): 635; author reply 637
- Grawe B, Schroeder AJ, Kakazu R, Messer MS: Lateral collateral ligament injury about the knee: Anatomy, evaluation, and management. *J Am Acad Orthop Surg*, 2018; 26(6): e120–27
- Numata H, Nakase J, Kitaoka K et al: Two-dimensional motion analysis of dynamic knee valgus identifies female high school athletes at risk of non-contact anterior cruciate ligament injury. *Knee Surg Sports Traumatol Arthrosc*, 2018; 26(2): 442–47
- Gialain IO, Coto NP, Driemeier L et al: A three-dimensional finite element analysis of the sports mouthguard. *Dent Traumatol*, 2016; 32(5): 409–15
- Ohyama T, Yasuda H, Shibuya N et al: Three-dimensional finite element analysis of the effects of implant diameter and photofunctionalization on peri-implant stress. *J Oral Sci*, 2017; 59(2): 273–78
- Carpenter RD: Finite element analysis of the hip and spine based on quantitative computed tomography. *Curr Osteoporos Rep*, 2013; 11(2): 156–62
- Akrami M, Craig K, Dibaj M et al: A three-dimensional finite element analysis of the human hip. *J Med Eng Technol*, 2018; 42(7): 546–52
- Tan B, Li N, Feng Z et al: [Construction of three-dimensional finite element model and biomechanical study on patient with with cervical spondylosis myelopathy]. *Zhong Nan Da Xue Xue Bao Yi Xue Ban*, 2019; 44(5): 507–14 [in Chinese]
- He C, He W, Li Y et al: Biomechanics of knee joints after anterior cruciate ligament reconstruction. *J Knee Surg*, 2018; 31(4): 352–58
- Wan C, Hao Z, Wen S: The effect of healing in the medial collateral ligament of human knee joint: A three-dimensional finite element analysis. *Proc Inst Mech Eng H*, 2016; 230(9): 867–75
- Pena E, Calvo B, Martinez MA, Doblare M: A three-dimensional finite element analysis of the combined behavior of ligaments and menisci in the healthy human knee joint. *J Biomech*, 2006; 39(9): 1686–701

## Conclusions

We compared the biomechanics of the knees of sheep and mini-pigs by systematic development of tissue structural models, followed by calculations from finite element analysis. Our results verified that the stress values of the cartilage, meniscus, and peripheral ligaments in the knee joint of the mini-pig were more similar to those of human knees [31,32]. The differences in stress peaks and changes under conditions of flexion in the sheep and mini-pig knees are mainly caused by inter-species differences, but intra-species differences may also be present.

## Conflicts of interest

None.